Unveiling Structural, Electronic, Mechanical and Optical Properties of $LiTaO_3$ for Potential Optoelectronic Applications by Density Functional Theory

Mita Chakraborty; Md. Rajib Munshi; Md Al Masud
Department of Physics, European University of Bangladesh
Department of IPE, European University of Bangladesh

Abstract:
Applying density functional theory different physical aspects of $LiTaO_3$ perovskite including structural, electronic, mechanical and optical properties have been analyzed by Generalized Gradient Approximation with PBE and RPBE approaches. $LiTaO_3$ crystal posses' indirect bandgap values of 2.24 and 2.27 eV respectively in PBE and RPBE techniques. Through density of states variety of nature and contribution of atomic orbital in $LiTaO_3$ crystal were studied. The analysis of Mulliken population charge revealed important details regarding the bonding features of $LiTaO_3$ crystal. The verification of mechanical stability was conducted through the application of the Born stability criterion, while Poisson's ratio and Pugh's ratio were analysed to evaluate ductile strength and elastic anisotropy. The $LiTaO_3$ crystal exhibits notable mechanical and thermal stability, as well as ductile characteristics and elastic anisotropy. The optical properties were meticulously assessed with an emphasis on energy and wavelength, and both methods validated that $LiTaO_3$ crystal exhibits the potentiality for strong contender in optoelectronics and photocatalytic applications.

Keywords: Electronic structure, DOS, PDOS, Mechanical, Optical, Optoelectronic.

Introduction

Natural gas, gasoline, and biofuels are mostly utilized for generating electricity, supplying heat, and powering transportation systems [1-2]. Nevertheless, if they are kept in use, they will continue to harm the environment and drain precious resources. Scholars are working tirelessly to find new energy sources and improve upon existing ones by expanding the frontiers of material science and discovering innovative materials [3-5]. To address the increasing global energy demand, it is crucial to do this study continuously in order to find sustainable solutions. "A" stands for alkaline earth metals like Li, Cs, Ca, Sr etc, "B" for transition or rare-earth metals like Ti, Mn, Fe, V, Ta, Nb; and "O" for the oxide ion; the ABO_3 formula is commonly used to describe oxide-perovskites. Perovskite materials are very compatible with current economic infrastructures and are inexpensive [6-7]. Computational methods have recently advanced to the point that many more material properties, including electrical, magnetic, and mechanical ones, may be evaluated. The correctness of these computational approaches is supported by the remarkable correlation between their results and experimental data [8]. Theoretical investigations of several semiconductors, such as $KTaO_3$, $KNbO_3$,

DOI: https://doi.org/10.5281/zenodo.15567727

$CsTaO_3$, etc., have focused heavily on these materials because of their high photocatalytic activity and huge surface areas [9–11]. Although many are interested in the potential uses of Ta and its derivatives, $LiTaO_3$ has not received much attention in this field. There must be a comprehensive scientific evaluation of $LiTaO_3$ before its technical implementation [12]. Theoretical investigations of these aspects using first-principles computation have also shown to be highly effective [13–14]. So far, the physical properties of $LiTaO_3$ have received minimal attention from scientists. We dug further into $LiTaO_3$ crystal and collected further data on its physical properties in an effort to address this knowledge gap. We addressed several physical properties of the $LiTaO_3$ crystal adopting Perdew Burke Ernzerhof (PBE) and Revised Perdew Burke Ernzerhof (RPBE). Future experimental investigations should be considerably aided by our study, which will lead to improved understanding of this material for future world.

Computational details

To accomplish very accurate computations, this work used 6 × 6 x 6 k-point mesh and pseudopotentials with a 500 eV cutoff energy [15]. Achieving overall energy convergence to within 0.2000×10^{-4} eV/atom was the result of structural optimization performed using the BFGS method. Furthermore, an ionic force of 0.5000×10^{-1} eV/Å was recorded, an ionic displacement of 0.2000×10^{-2} Å, and a stress component of 0.1000 GPa achieved.

Results and discussion

Structural analysis

Starting with a lattice parameter of 3.89 Å and angles $\alpha = \beta = \gamma = 90°$, the structural refinement of $LiTaO_3$ crystals was initiated. In terms of space group $Pm\bar{3}m$, the optimized $LiTaO_3$ crystal takes on a cubic form [221]. The point group Pm3m and the Hall symbol -P 423, which belong to the crystal, provide further crystallographic details. The ideal $LiTaO_3$ combinations are summarized in Table 1 and Figure 1 shows the crystal structure of the cubical $LiTaO_3$.

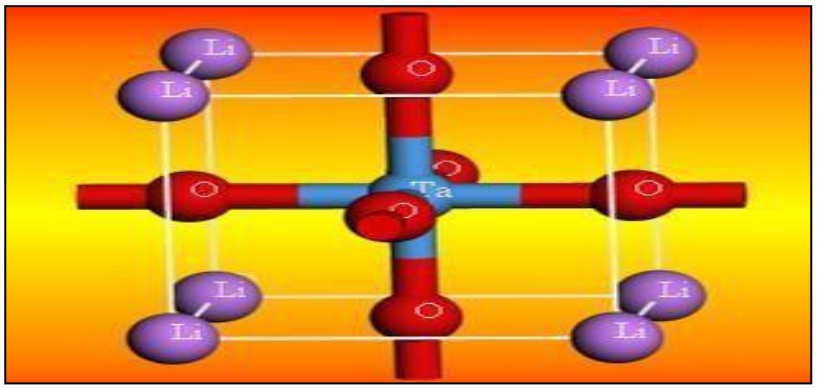

Figure 1 Crystal structure of $LiTaO_3$

DOI: https://doi.org/10.5281/zenodo.15567727

Table 1 Final energy, cell volume and lattice parameter of $LiTaO_3$ crystal

Material Name	Final Energy (eV)	Cell volume ($Å^3$)	attice constant a=b=c (Å)	Approaches
$LiTaO_3$	-46.405426800	6.854298	3.8452192	PBE
	-47.646209197	57.180456	3.852558	RPBE

Electronic band structure

According to band structure, specifically their band gap energy, materials are categorized as insulators, semiconductors, or metals [16–17]. From Figures 2 (a) and 2 (b), $LiTaO_3$ crystal is found to be a semiconductor by calculating its narrow indirect band gap utilizing techniques such as PBE and RPBE methods respectively while K points occurs from X-R-M-Γ-R and summarized in Table 2.

Table 2 Bandgap values of $LiTaO_3$ crystal

Bandgap Value (eV)	Techniques Name
2.24	PBE
2.27	RPBE

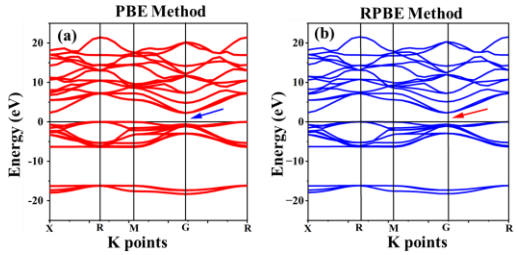

Figure 2 Band structure of $LiTaO_3$ by (a) PBE, (b) RPBE methods respectively

The distribution of energy level in a material and separation of occupied states from unoccupied is clarify using density of states (DOS) plot [18-19]. The semiconductor nature is improved by the variation of different energy band by illustrating DOS and PDOS of $LiTaO_3$ in Figure 3 (a, b) for both methods, where maximum density of states in valence and conduction band reaches 5.0 and 4.0 electrons/eV.

The PDOS analysis presented in Figure 4 (a, b) reveals that within the valence band, the Li atom little contributed via the s orbital, while the Ta atom contributes through the s, p and d orbitals. Finally, the O atom primarily contributes through the s, p orbital [20]. The primary contributions in the conduction band stem from the Li-s, Ta-d, and O-p orbitals. The major peak in valence band composed by Ta-s/p/d and and O-s/p orbitals. The notable peak in conduction band arises due to combined effect of Li-s, Ta-p/d and O-p orbitals.

DOI: https://doi.org/10.5281/zenodo.15567727

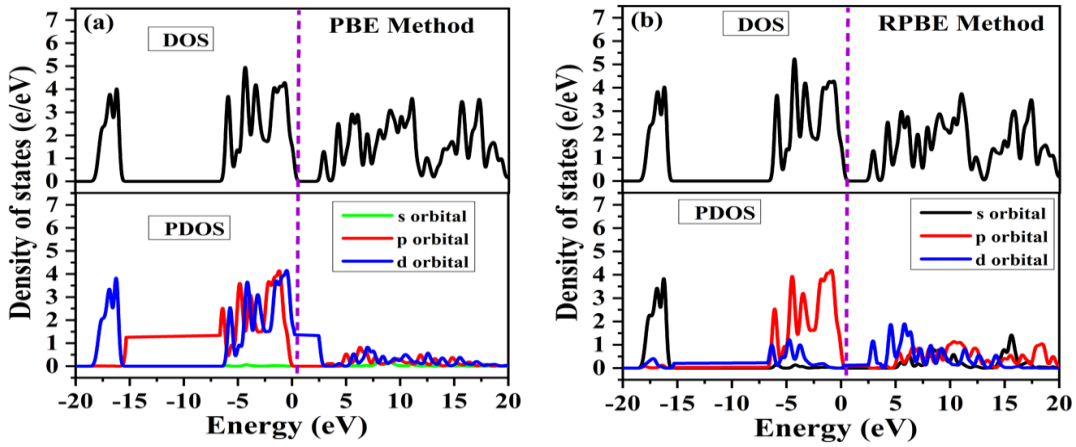

Figure 3 DOS and PDOS of $LiTaO_3$ crystal

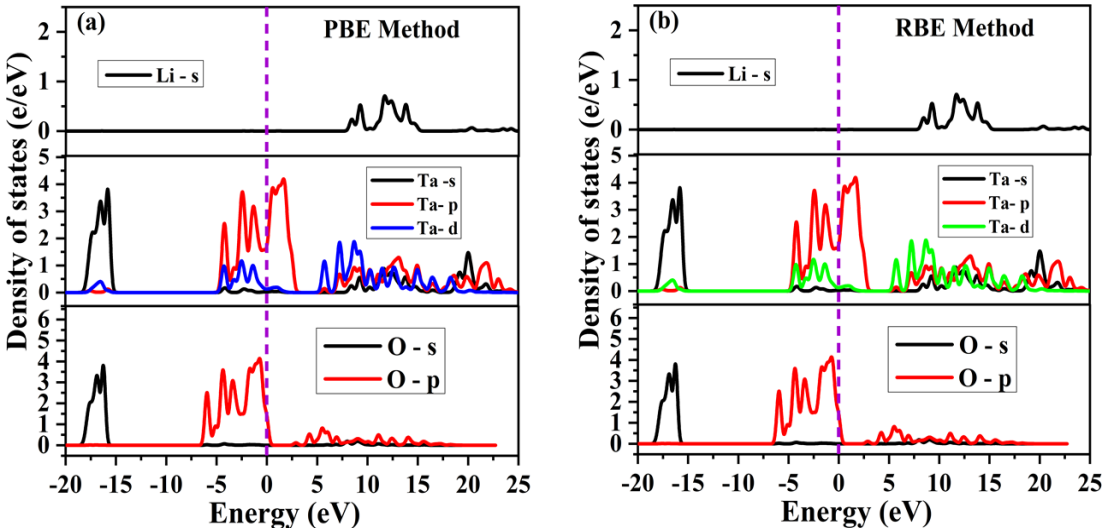

Figure 4 Different states of Li, Ta and O atom.

Mechanical Properties

For mechanical stability, every cubic perovskite must fill-up the stability criteria of Born, as outlined in [22]: $C_{11}> 0$, $C_{44}> 0$, $C_{11}-C_{12}> 0$, and $C_{11}+2C_{12}> 0$.

The mechanical properties of $LiTaO_3$, as assessed through PBE and RPBE methods, are presented in Table 3, confirming its stability under specific conditions.

The response of the material to stress-induced volume variations can be analyzed through the calculation of the Cauchy pressure, defined as C_{12}-C_{44}. A positive Cauchy pressure signifies ductility and metallic bonding, while a negative Cauchy pressure indicates brittleness and the existence of directed bonding, including covalent or partly ionic contacts. The negative estimated value of $LiTaO_3$ indicates strong directional bonding, such as covalent or partially ionic interactions, and implies a brittle nature.

Additionally, Pugh's ratio B/G, a reliable indicator of mechanical pliability or brittleness, was used to evaluate the ductile or brittle behavior of the material. An indicative ratio of B/G>1.75 suggests ductile behavior according

DOI: https://doi.org/10.5281/zenodo.15567727

to this standard, whereas B/G<1.75 implies brittleness. The computed value of Pugh for $LiTaO_3$ is 1.40, which is below the critical value, suggesting that the material exhibits brittle mechanical behavior. The consistency of Pugh's ratio and Cauchy pressure lends strong support to these findings. High bulk modulus (B) values signify strong elasticity, incompressibility, and stiffness, which are characteristic of $LiTaO_3$ and elevated Young's modulus of $LiTaO_3$ denotes its stiffness, rigidity, and resistance to deformation under tensile or compressive stress, reflecting robust mechanical stability. The shear modulus (G) demonstrates a significant resistance to shear deformation, thereby ensuring the stability of structures [23]. Materials with a Poisson's ratio below 0.5 often possess robust atomic or molecule bonding, since they exhibit resistance to deformation while still experiencing lateral contraction or expansion under tensile or compressive forces, with diminishing strength as the ratio approaches 0.5. The atomic and molecular interactions of $LiTaO_3$ are robust, as indicated by the assessed Poisson's ratios of 0.21 and 0.20 in both approaches. The strong rigidity and mechanical stability of the cubic $LiTaO_3$ crystal evidenced by the moderate anisotropy values of 0.88 and 0.90 obtained through both methods for the universal anisotropy index [24].

Table 3 Values of elastic constants and otherparameter of $LiTaO_3$ crystal.

Techniques Name	C_{11}	C_{12}	C_{44}	C_{12}-C_{44}	B	Y	G	B/G	ν	A
PBE	**506.72**	41.59	**75.39**	**- 33.80**	**196.63**	**336.03**	**138.26**	**1.42**	**0.21**	**0.88**
RPBE	**495.29**	**48.02**	**96.11**	**-48.09**	**197.11**	**353.43**	**147.12**	**1.33**	**0.20**	**0.90**

Optical properties:

All computational approaches used a 0.1 eV Gaussian smearing to examine the optical characteristics of $LiTaO_3$ crystal. Reflection measurements presented in Figure 5 (a, b) demonstrate a notable increase from 1.0 eV to 23 eV, with all methods indicating peak reflectivity only around 0.78 eV in both PBE and RBE approaches. The energy loss function, an essential parameter for enhancing energy efficiency in optoelectronics, is illustrated in Figure 5 (c, d). Results indicate that the $LiTaO_3$ crystal exhibits lower energy loss in both methods, with the PBE method yielding lower values than the RPBE method.

DOI: https://doi.org/10.5281/zenodo.15567727

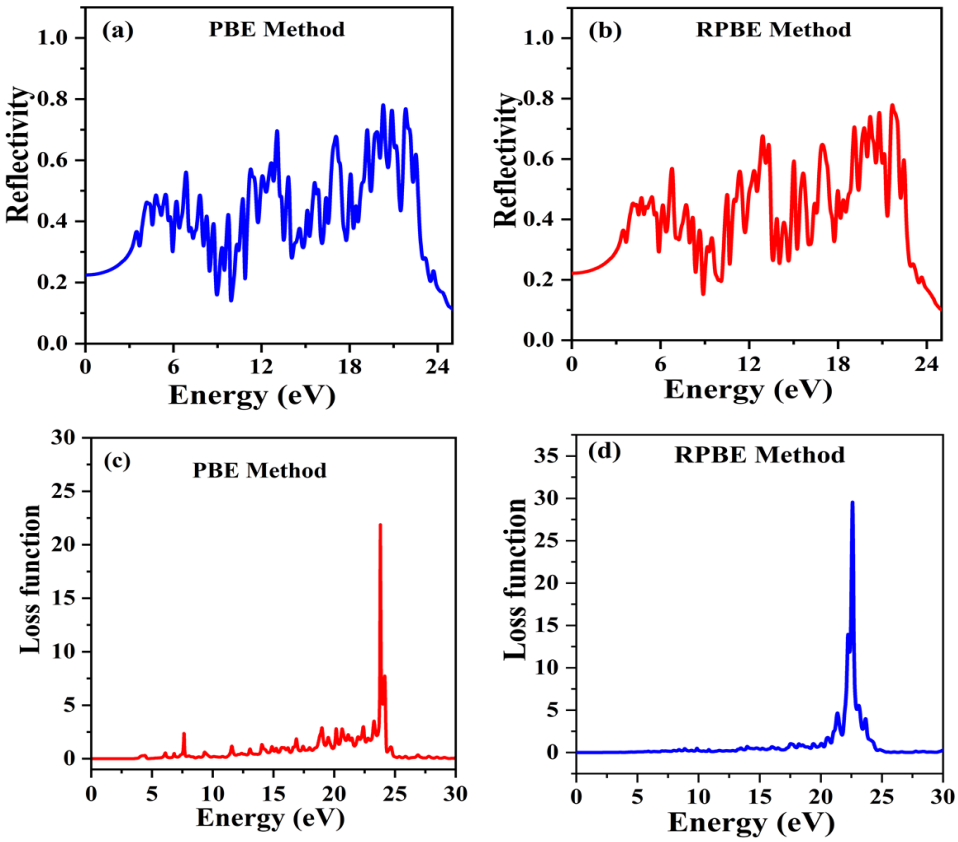

Figure 5 (a, b) Optical reflectivity, (c, d) Loss function

Optical conductivity reflects a material's ability to transmit visible light, with the real component indicating conductivity and the imaginary component representing energy dissipation [31]. As shown in Figure 6 (a, b), real component surpasses the imaginary component between 2.5 and 11.0 eV, then gradually decreases by 25 eV. Conversely, the imaginary component dominates from 10.0 to 25.0 eV, highlighting variations in energy absorption and conductivity.

Dielectric functions are essential for comprehending optical behavior and for the design of tailored blends [32]. Figure 6 (c, d) illustrates that the real part of $LiTaO_3$ predominates over the imaginary part from 0 to 5.0 eV, subsequently decreasing up to 25.0 eV. In the energy range of 5.0 to 25.0 eV, the imaginary component surpasses the real component, signifying considerable absorption in the presence of an electric field.

DOI: https://doi.org/10.5281/zenodo.15567727

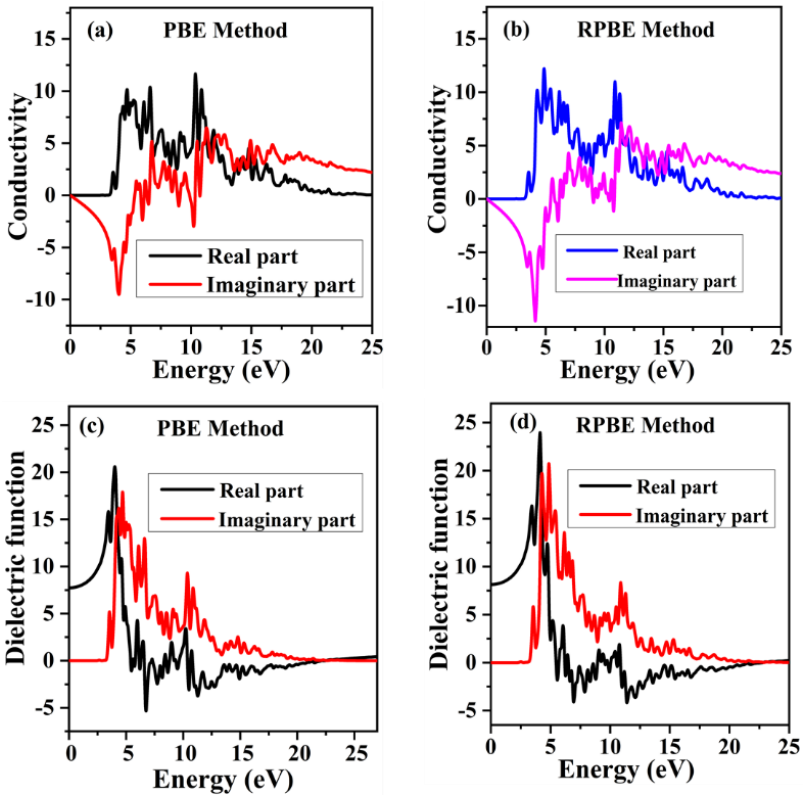

Figure 6 (a, b) Conductivity and (c, d) Dielectric function

The inspection of the refractive index in Figure 7 (a, b) demonstrates an inverse relationship between the real and imaginary components in both techniques [33]. Between 0 and 5 eV, the real component of the refractive index surpasses the imaginary component, signifying predominant refractive characteristics and little absorption. In the 5 to 25 eV region, the imaginary component exceeds the real portion, indicating significant absorption. This result indicates that $LiTaO_3$ has increased optical absorption in the higher energy spectrum, which substantially affects its optical characteristics and renders it appropriate for applications like optical filters and protective coatings.

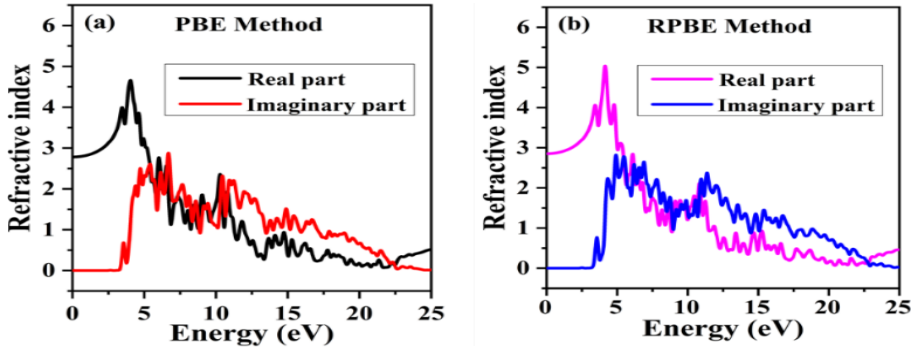

Figure 7 (a, b) Refractive index of $LiTaO_3$ crystal

DOI: https://doi.org/10.5281/zenodo.15567727

The absorption spectra of $LiTaO_3$ depicted in Figure 8(a, b), exhibit a uniform trend ranging from 0 to 25 eV, as established through the application of the PBE and RPBE, methodologies. In the visible spectrum (1.78–4.14 eV or 300–700 nm), the material exhibits notable absorption, with a peak observed at 3.76 eV across all utilized techniques [34-35].

Additionally, the ultraviolet (UV) spectrum displays a variety of absorption peaks, with the most significant peak identified at 11.0 eV. This action emphasizes the exceptional and extensive optical absorption properties of $LiTaO_3$ by showcasing its effectiveness in absorbing light across the visible and ultraviolet spectrums [36].

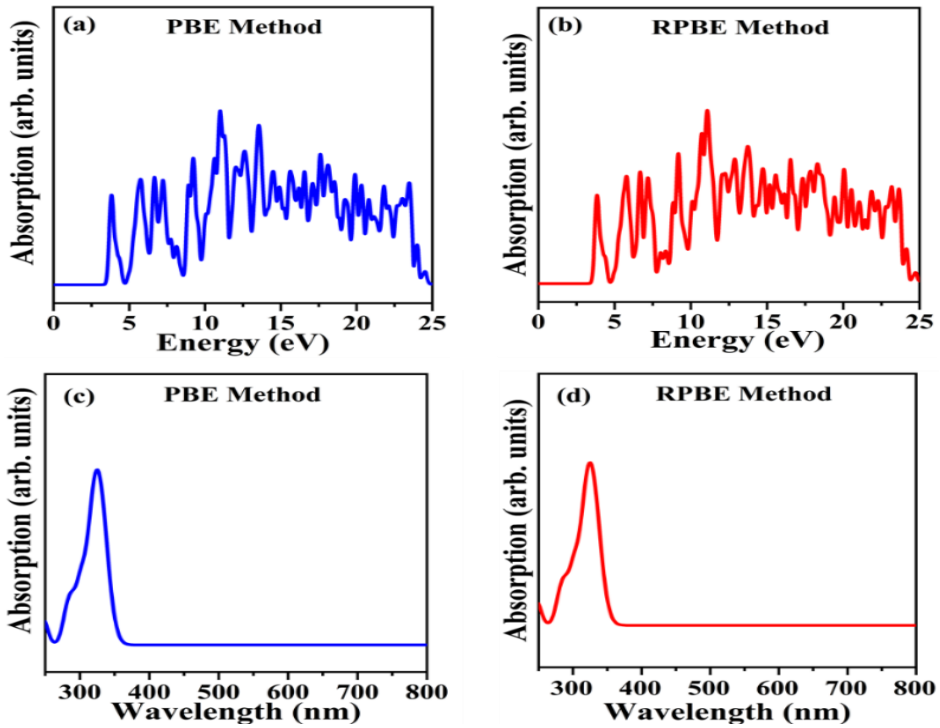

Figure 8. Optical absorption (a, b) against energy (eV) and (c, d) wavelength (nm)

Furthermore, the absorption coefficient curves of $LiTaO_3$ against wavelength are presented in Figures 8 (c, d) respectively. Throughout the visible spectrum (300 to 700 nm), the data illustrates distinct absorption peaks. The peak absorption for both methods observed near 325 nm. The wavelengths identified align with the areas where $LiTaO_3$ demonstrates maximum light absorption, underscoring its significant absorption characteristics at these particular wavelengths. Furthermore, the absorption characteristics observed in the visible spectrum demonstrate that $LiTaO_3$ shows considerable sensitivity to visible light, implying its possible applications in fields such as optoelectronics and photocatalysis, where accurate light control and detection are essential [37].

Conclusion:

Exploring structural, electrical, elastic, and optical phenomena of cubic $LiTaO_3$ crystals conducted by first principle simulations. The band gap energies (Eg) estimated using the PBE, RPBE, functional successively reveal an indirect bandgap with values of 2.24 eV, 2.27 eV. Mulliken population study was conducted to better grasp the bonding characteristics of $LiTaO_3$. The exceptional mechanical stability of the material, together with its great ductility elastic anisotropies of $LiTaO_3$ are visualized and discussed, indicating that it can easily

DOI: https://doi.org/10.5281/zenodo.15567727

resist mechanical stress. Furthermore, the high value of Young's and Shear modulus of this crystal are anticipated. $LiTaO_3$ crystals may serve as outstanding candidates for advancing optoelectronic and photocatalytic applications in the future for suitable bandgap and absorption capabilities.

Acknowledgments
The authors acknowledge the Department of Physics and ICT, European University of Bangladesh, Dhaka-1216, for providing facilities and support to carry out this work.

Disclosure of conflict of interest
The authors hereby declare there is no conflict of interest.

References:

[1] Deng M, Shen S, Wang X, Zhang Y, Xu H, Zhang T, Wang Q. Controlled synthesis of $AgInS_2$ nanocrystals and their application in organic–inorganic hybrid photodetectors. Cryst Eng Comm. 2013,15, 6443.

[2] Sen S k, Munshi M R, Kumar A, Mortuza A. A, Manir M S, Islam M A, Hossain M N, Hossain M K, Structural, optical, magnetic, and enhanced antibacterial properties of hydrothermally synthesized Sm-incorporating α-MoO_3 2D-layered nanoplates. *RSC advances*, 2022, *12*,34584-34600.

[3] Liu Y, Zhang W, Wang B, Sun L, Li F, Xue Z, Nian H. Theoretical and experimental investigations on high temperature mechanical and thermal properties of $BaZrO_3$. Ceramic International, 2018, 44, 16475-16482.

[4] Feng, Zhenbao, Haiquan H, Shouxin C, Bai C. First-principles study of optical properties of $SrZrO_3$ in cubic phase. Solid State Communication, 2008, 148: 472-475.

[5] Islam M T, Kumar, A, Chakma U, Howlader, D. A computational investigation of electronic structure and optical properties of $AlCuO_2$ and $AlCu_{0.96}Fe_{0.04}O_2$: a first principle approach. Orbital: The Electronic Journal of Chemistry, 2021,13(1), 58-64.

[6] Amisi S, Bousquet E, Katcho K, Ghosez P. First-principles study of structural and vibrational properties of $SrZrO_3$. Physical Review B**,** 2012, *85*, 064112.

[7] Kang S G, Sholl D S. First-principles investigation of chemical stability and proton conductivity of M-doped $BaZrO_3$ (M= K, Rb, and Cs). Journal of American Ceramic Society, 2017, *100*, 2997-3003.

[8] Liu Q J, Liu Z T, Feng L P, Tian H. Mechanical, electronic, chemical bonding and optical properties of cubic BaHfO3: First-principles calculations, Physica B, 2010 ,405, 4032–4039.

[9] Xu Y Q, Wu S Y, Zhang L J, Wu L N, Ding C C, First-principles study of structural, electronic, elastic, and optical properties of cubic $KNbO_3$ and $KTaO_3$ crystals, journal, 2016, 254 (5), 1600620.

[10] Sarwan M, Shukla P, Singh S, Structural stability, electronic and elastic properties of cubic $RbTaO_3$ perovskite oxide, *AIP Conf. Proc.* 2020, 2265, 03034

[11] Eyi E E, Ece Eyi, Ab initio study of the structural, electronic and optical properties of $NaTaO_3$, Philosophical Magazine, 2010, 90(21), 2965–2976.

[12] Khenata R, Sahnoun M, Baltache H, Rérat M, Rashek A H, Illes N, Bouhafs B. First-principle calculations of structural, electronic and optical properties of $BaTiO_3$ and $BaZrO_3$ under

DOI: https://doi.org/10.5281/zenodo.15567727

hydrostatic pressure**.** Solid State Communication**.,** 2005, *136*, 120-125.

[13] Adewale A A, Chik A, Adam T, Yusuff O K, Ayinde S A, Sanusi Y K. First principles calculations of structural, electronic, mechanical and thermoelectric properties of cubic $ATiO_3$ (A= Be, Mg, Ca, Sr and Ba) perovskite oxide. Computational Condense Matter, 2021, *28*, e00562.

[14] Muscat J, Wander A, Harrison N M. On the prediction of band gaps from hybrid functional theory. Chemical Physics Letter, 2001, 342, 397–401.

[15] Rizwan M, Aleena S, Shakil M, Mahmood T, Zafar A A, Hussain T, Farooq M H. A computational insight of electronic and optical properties of Cd-doped $BaZrO_3$. Chineese journal of Physics, 2020, *66*, 318-326.

[16] Zahan M S, Munshi M R, Rana M Z, Masud M A. Theoretical insights on geometrical, mechanical, electronic, thermodynamic and photocatalytic characteristics of $RaTiO_3$ compound: A DFT investigation. Computational Condense Matter, 2023, 1, 36: e00832.

[17] Munshi M R, Masud M A, Khatun A. Structural, electronic, mechanical, thermodynamic and optical properties of oxide perovskite $BeZrO_3$: a DFT study, *Physica Scripta*, 2024 , 99 (8), 085904.

[18] Munshi M R, Rana M Z, Sen S K, Foisal M R A, Ali M H. Theoretical investigation of structural, electronic, optical and thermoelectric properties of $GaAgO_2$ based on Density Functional Theory (DFT): Two approach. World Journal of Advance Research and Review, 2022, 13, 279–291.

[19] Haoui A, Elchikh M, Hiadsi S. Mechanical, optoelectronic and thermoelectric properties of the transition metal oxide perovskites $YScO_3$ and $LaScO_3$: first principle calculation, Physica B: Condensed Matter, 2023, 654, 414732.

[20] Munshi M R , Sen S K, Rana M Z. Electronic, thermodynamic, optical and photocatalytic properties of $GaAgO_2$ and $AlAgO_2$ compounds scrutinized via a systemic hybrid DFT, Computational Condense Matter, 2023 , 34, e00778.

[21] Rana M Z , Munshi M R , Masud M A, Zahan M S. Structural, electronic, optical and thermodynamic properties of $AlAuO_2$ and $AlAu0_{.94}Fe_{0.06}$ O_2 compounds scrutinized by density functional theory (DFT). Heliyon, 2023, 9 ,11.

[22] Rahman N, Husain M,Yang J, Sajjad M, Murtaza G, Haq M U, Habib A, Zulfiqar, Rauf A, Karim A, Nisar M, Yaqoob M, Khan A. First principle study of structural, electronic, optical and mechanical properties of cubic fluoro-perovskites: ($CdXF_3$, *X* = *Y*, Bi). European Physical Journal Plus, 2021, 136, 347.

[23] Sohail M, Hussain M, Rahman N, Althubeiti K, Algethami M, Khan A A, Iqbal A, Ullah A, Khan A, Khan R. First-principal investigations of electronic, structural, elastic and optical properties of the fluoro perovskite TlLF3 (L = Ca, Cd) compounds for optoelectronic applications. RSC Advances, 2022 , 12, 7002-7008.

DOI: https://doi.org/10.5281/zenodo.15567727

[24] Qaisi S A , Mebed A M , Mushtaq M , Rai D P , Alrebdi T A, Sheikh R A, Rached H , Ahmed R , Faizan M, Bouzgarrou S, Javed M A. A theoretical investigation of the lead-free double perovskites halides Rb_2XCl_6 (X= Se, Ti) for optoelectronic and thermoelectric applications. Journal of Computational Chemistry, 2023, 44(19), 690-1703.

[25] Kaufman L, Cohen M. Thermodynamics and kinetics of martensitic transformations. Progress in Physics of Metals, 1958, 7, 165–246.

[26] Rahman S, Hussain A, Noreen S, Bibi N, Arshad S, Rehman J U, Tahir M B. Structural, electronic, optical and mechanical properties of oxide-based perovskite ABO_3 (A = Cu, Nd and B = Sn, Sc): A DFT study. Journal of Solid State Chemistry, 2023, 317, 123650.

[27] Rehman J U , Usman M , Tahir M B, Hussain A , Rashid M. Investigation of Structural, Electronics, Optical, Mechanical and Thermodynamic Properties of YRu_2P_2 Compound for Superconducting Application. Journal of Superconductivity and Novel Magnetism, 2021, 34, 3089–3097.

[28] Colmenero F., Timón V., 2018 Study of the structural, vibrational and thermodynamic properties of natroxalate mineral using density functional theory. J. Solid State Chem. 263, 131–140.

[29] Ferrari A M, Orlando R, Rérat M. Ab Initio Calculation of the Ultraviolet–Visible (UV-vis) Absorption Spectrum, Electron-Loss Function, and Reflectivity of Solids. Journal of Chemical Theory and Computation, 2015,11, 3245–3258.

[30] Islam M A, Islam J, Islam M N, Sen S K, Hossain A K M A. Enhanced ductility and optoelectronic properties of environment-friendly $CsGeCl_3$ under pressure. AIP Advances, 2021, 11, 045014.

[31] Kora H H, Taha M, Abdelwahab A, Farghali A A, El-dek S I. Effect of pressure on the geometric, electronic structure, elastic, and optical properties of the normal spinel $MgFe_2O_4$: a first-principles study. Materials Research Express, 2020, 7, 106101.

[32] Qaisi S A , Mushtaq M, Alzahrani J S, Alkhaldi H, Alrowaili Z A, Rached H, Haq B U, Mahmood Q, Buriahi M S A, Morsi M. First-principles calculations to investigate electronic, structural, optical, and thermoelectric properties of semiconducting double perovskite Ba_2YBiO_6. Micro and Nanostructures, 2022, 170, 207397.

[33] Dey A, Sharma R, Dar S A, Wani I H. Cubic $PbGeO_3$ perovskite oxide: a compound with striking electronic, thermoelectric and optical properties, explored using DFT studies. Computational Condensed Matter, 2021, 26, e00532.

[34] Munshi M R, Zahan M S, Rana M Z, Masud M, A. First principles prediction of structural, electronic, mechanical, thermodynamic, optical and photocatalytic properties of $In(X)O_2$, where X= Cu, Ag crystal scrutinized by density functional theory. Computational Condensed Matter, 2024, 38, e00884.

[35] Rahman S, Hussain A, Noreen S, Bibi N., Arshad S, Rehman J U, Tahir M B. Structural, electronic, optical and mechanical properties of oxide-based perovskite ABO_3 (A= Cu, Nd and B= Sn, Sc): A DFT study. Journal of Solid State Chemistry, 2023, 317,123650.

DOI: https://doi.org/10.5281/zenodo.15567727

[36] Munshi M R, Masud M A, Rahman M, Khatun M R, Mian M F. First principles prediction of geometrical, electronic, mechanical, thermodynamic, optical and photocatalytic properties of $RaZrO_3$ scrutinized by DFT investigation, Computational Condensed Matter, 2024, 38.

[37] Babu K E, Veeraiah A, Swamy D T, Veeraiah V. First-principles study of electronic and optical properties of cubic perovskite $CsSrF_3$, Material science Poland, 2012, 30, 359-67.

DOI: https://doi.org/10.5281/zenodo.15567727